ELSEVIER

Neurobiology of Disease

www.elsevier.com/locate/ynbdi
Neurobiology of Disease 25 (2007) 571 – 581

Preventing polyglutamine-induced activation of c-Jun delays neuronal dysfunction in a mouse model of SCA7 retinopathy

Karine Merienne,[a,b,*] James Friedman,[c] Masayuki Akimoto,[c,e] Gretta Abou-Sleymane,[a,b] Chantal Weber,[a,b] Anand Swaroop,[c,d] and Yvon Trottier[a,b,*]

[a]*Department of Molecular Pathology, Institut de Génétique et Biologie Moléculaire et Cellulaire (IGBMC), CNRS/INSERM/ULP, BP10142, 67404 Illkirch Cédex, CU de Strasbourg, France*
[b]*Chaire de Génétique Humaine, Collège de France, France*
[c]*Departments of Ophthalmology and Visual Sciences, University of Michigan, Ann Arbor, MI 48105, USA*
[d]*Department of Human Genetics, W.K. Kellogg Eye Center, University of Michigan, Ann Arbor, MI 48105, USA*
[e]*Translational Research Center, Kyoto University Hospital, Japan*

Received 4 July 2006; revised 27 October 2006; accepted 1 November 2006
Available online 26 December 2006

We have approached the role of cellular stress in neurodegenerative diseases caused by polyglutamine expansion (polyQ) in the context of Spinocerebellar ataxia type 7 (SCA7) that includes retinal degeneration. Using the R7E mouse, in which polyQ-ataxin-7 is specifically over-expressed in rod photoreceptors, we previously showed that rod dysfunction correlated to moderate and prolonged activation of the JNK/c-Jun stress pathway. SCA7 retinopathy was also associated with reduced expression of rod-specific genes, including the transcription factor Nrl, which is essential for rod differentiation and function. Here, we report that R7E retinopathy is improved upon breeding with the JunAA knock-in mice, in which JNK-mediated activation of c-Jun is compromised. Expression of Nrl and its downstream targets, which are involved in phototranduction, are partially restored in the JunAA-R7E mice. We further show that c-Jun can directly repress the transcription of Nrl. Our studies suggest that polyQ-induced cellular stress leads to repression of genes necessary for neuronal fate and function.

Keywords: Polyglutamine expansion; Neuronal stress; JNK/c-Jun pathway; Retina; Nrl; Photoreceptor; Gene regulation

Introduction

Nine autosomal dominant neurodegenerative disorders, characterized by dysfunction and/or degeneration of distinct neurons, are caused by expansion of CAG trinucleotide repeats. This expansion results in a longer polyQ-track, which in turn leads to toxic gain-of-function and increased propensity of the expanded protein to aggregate (Scherzinger et al., 1997; Ross and Poirier, 2004). Consequently, the hallmarks of polyQ disorders are nuclear inclusions (NIs) containing aggregated mutant proteins in affected neurons (Di Figlia et al., 1997; Paulson et al., 1997; Skinner et al., 1997). Although toxicity of NIs *per se* can be debated, a number of studies suggest deregulation of cellular components involved in folding and/or degradation of proteins as a possible mechanism of disease pathogenesis (Warrick et al., 1999; Bence et al., 2001; Miller et al., 2005; Vacher et al., 2005; Waza et al., 2005). Protein misfolding is expected to induce cellular stress response, including the activation of the JNK/ cJun/AP-1 signaling pathway (Sherman and Goldberg, 2001; Nishitoh et al., 2002; Merienne et al., 2003; Garcia et al., 2004). In addition, excitotoxicity, energy impairment, defects in calcium homeostasis and oxidative stress, which are also stress responses associated with activation of JNK/ AP-1 pathway, are implicated in polyQ expansion diseases (Browne et al., 1997; Lin et al., 2000; Wyttenbach et al., 2002; Li et al., 2003; Seong et al., 2005).

Activator protein 1 (AP-1) is a key transcriptional regulator of diverse cellular events, including those implicated in cell survival, death, proliferation and differentiation (Shaulian and Karin, 2001). Depending on the context, intensity, duration of the stimulus, stage of differentiation and cell type, AP-1 can promote one path or another. In mature neurons, activation of AP-1 causes death in response to short and acute stress (Yang et al., 1997; Behrens et al., 1999; Whitfield et al., 2001). PolyQ expansion induces moderate but sustained activation of AP-1 in mouse models (Merienne et al., 2003); however, the contribution of AP-1 to pathogenesis of polyQ diseases has not yet been elucidated.

Spinocerebellar ataxia type 7 (SCA7) is unique among polyQ diseases since the clinical phenotype also includes retinal degenera-

* Corresponding authors. Department of Molecular Pathology, Institut de Génétique et Biologie Moléculaire et Cellulaire (IGBMC), CNRS/INSERM/ULP, BP10142, 67404 Illkirch Cédex, CU de Strasbourg, France. Fax: +33 3 88653246.
E-mail addresses: merienne@igbmc.u-strasbg.fr (K. Merienne), yvon@igbmc.u-strasbg.fr (Y. Trottier).
Available online on ScienceDirect (www.sciencedirect.com).

0969-9961/$ - see front matter © 2006 Elsevier Inc. All rights reserved.
doi:10.1016/j.nbd.2006.11.002

tion and eventually blindness. The retina is relatively less complex yet most approachable part of the central nervous system (Dowling, 1987). Photoreceptors account for over 70% of retinal cells in humans and mice; of these, 95-97% are rods. Mutations in phototransduction genes and their transcriptional regulators are associated with photoreceptor degeneration, thus allowing direct correlations between gene mutation and cell function (Molday, 1998; Rattner et al., 1999; Pacione et al., 2003). To decipher the molecular basis of polyQ toxicity, we developed a SCA7 transgenic mouse model–R7E–to specifically target rod photoreceptors using the rhodopsin promoter (Yvert et al., 2000). This mouse model reproduced the primary features of SCA7 pathology, including progressive functional alteration, followed by rod degeneration. Other SCA7 models with retinopathy include the transgenic mice expressing polyQ-ataxin-7 using a prion protein promoter (La Spada et al., 2001) and the *SCA7* knock-in mice (Yoo et al., 2003).

Recent studies have revealed that ataxin-7 is an integral component of the TFTC transcriptional complex (Helmlinger et al., 2004c). Although the transcriptional function of ataxin-7 in SCA7 disease remains to be elucidated, molecular clues of retinal pathology have been provided by the SCA7 mice. Accumulation of polyQ-ataxin-7 in the retina of these mice results in decreased expression of phototransduction genes [e.g., rhodopsin (*Rho*), rod transducin (*Gnat1*) and phosphodiesterase β (*Pdeb*)] (Yoo et al., 2003; Helmlinger et al., 2004b). The expression of rod-specific transcriptional regulators, including cone-rod homeobox (*Crx*) and neural retina leucine zipper (*Nrl*), is also reduced (La Spada et al., 2001; Chen et al., 2004b; Abou-Sleymane et al., 2006). As mutations in *CRX* and *NRL* lead to human retinal dystrophies (Freund et al., 1997; Sohocki et al., 1998; Bessant et al., 1999; Nishiguchi et al., 2004), SCA7 retinopathy may probably be a consequence of the reduced expression of phototransduction genes.

Using R7E transgenic mice, we have earlier shown that expression of polyQ-ataxin-7 in rods results in the activation of JNK/c-Jun/AP-1 stress signaling pathway (Merienne et al., 2003). Here, we have investigated the underlying mechanism of SCA7 retinopathy and the role of c-Jun/AP-1 by using a genetic approach. We show that the SCA7 retinopathy is modulated when R7E mice are mated with c-Jun deficient knock-in mice (JunAA), carrying a mutant Jun allele with alanine substitutions at serines 63 and 73, which can be phosphorylated by JNK (Behrens et al., 1999). We also demonstrate that *Nrl* and its target gene *Pdeb*, which are severely reduced in the R7E mice, are partially restored in the JunAA-R7E mice. Further biochemical studies suggest that AP-1 exerts a direct transcriptional control on *Nrl*, which is a bZIP transcription factor essential for rod photoreceptor differentiation and function (Swaroop et al., 1992; Mears et al., 2001). We propose that the cellular stress induced by polyQ expansion and mediated by AP-1 contributes to neurodegeneration by altering the expression of genes, which are required for neuronal function.

Materials and methods

Animals

Heterozygous R7E transgenic mice maintained in a C57BL/6 background (Yvert et al., 2000) were crossed with homozygous or heterozygous JunAA knock-in mice of mixed 129×C57BL/6×CBA background (kindly provided by E.F. Wagner). In JunAA mice, serine 63 and 73 of c-Jun are mutated to alanines. For genotyping, mouse tail DNA was screened by PCR as described (Behrens et al., 1999; Yvert et al., 2000). The matings were designed to generate litters for different groups to be compared (i.e. we crossed Junaa/aa with Junaa/wt-R7E and Junaa/wt with Junaa/wt-R7E animals). The experiments were approved by the ethical committee C.R.E.M.E.A.S (Comite Regional d'Ethique en Matiere d'Experimentation Animale de Strasbourg).

ERG

We conducted ERG testing as described (Helmlinger et al., 2002). Briefly, dark-adapted mice were anesthetized. Pupils were dilated, and the cornea was locally anesthetized. Scotopic rod ERGs were recorded in a Ganzfeld bowl, with light stimuli increasing from −4 to 1.4 log cd s m-2. Similarly, photopic cone ERGs were elicited with increasing light stimuli from −2 to 1.4 log cd s m-2, on a rod suppressing background after 6 min light adaptation. The duration of the light stimulus was constant. Responses were digitized using a data acquisition labmaster board. Responses were computer averaged at all intensities.

Immunohistofluorescence

Enucleated eyes were dissected to remove lens and cornea and fixed in fresh 4% paraformaldehyde for 2 h at 4°C. Fixed retinas were placed for 1 h in 30% sucrose, 1× PBS and frozen in OCT compound. Cryostat sections (10 μm) were permeabilized for 5 min with 0.1% Triton X-100, 1× PBS, blocked for 15 min with 0.5% bovine serum albumin, 0.1% Tween-20, 1× PBS. Primary antibodies used were rabbit polyclonal affinity-purified anti-ataxin-7 1261 at 1:100 (Yvert et al., 2000) and mouse monoclonal anti-rhodopsin 1D4 at 1:1000 (gift of D. Hicks). Primary and secondary antibodies (diluted to 1:200; anti-mouse CY3 and anti-rabbit Oregon green conjugated; Jackson ImmunoResearch Laboratories) were diluted in the blocking solution for 2 h at room temperature. Nuclei were counterstained with 0.5 μg/ml DAPI for 5 min. Quantification of segment thickness was performed by using Metamorph software (Universal Imaging). Briefly, retinal sections were cut from 4 WT, 4 JunAA, 3 CT-R7E and 3 JunAA-R7E mice. Sections cut at the same level within the retina were compared as follows: for each section, 3 measurements of segment thickness (always at the same level between the different sections) were performed and averaged.

Real-time RT-PCR analysis

Reverse transcription was performed on 1 μg of total retinal RNA using SuperScriptII (Invitrogen) and random hexamers according to the manufacturer instructions. We performed PCR amplifications of cDNA on a Light-Cycler instrument. PCR primers for detection of *Nrl*, *Crx, Rho, Gnat1, Pdeb, RhoK, Cyclophilin, 36B4* and recombinant *SCA7* mRNA are available upon request.

Western blotting analysis

Retinas were dissected and homogenized in lysis buffer containing 50 mM Tris-HCl pH 8.0, 10% glycerol, 5 mM EDTA, 150 mM KCl, 1 mM Pefabloc, a cocktail of protease inhibitors, 1 mM sodium fluorure, 1 mM sodium orthovanadate and 1% NP-40. They were incubated for 15 min on ice and centrifuged for

20 min at 13000 rpm and 4°C. Supernatants were collected and analysed on SDS-PAGE gels. To recover insoluble fractions, pellets were solubilized with formic acid, lyophilised, resuspended in SDS buffer (final concentration of 2% SDS, 5% β-mercaptoethanol, 15% glycerol) and analysed on SDS-PAGE, as described (Lunkes et al., 2002). Primary antibodies, rabbit polyclonal anti-Nrl (Swain et al., 2001), rabbit polyclonal anti-cJun sc45 (Santa Cruz Biotechnology), rabbit polyclonal anti-phospho-ser63-c-Jun antibody (Cell Signalling), rabbit polyclonal anti-phospho-JNK antibody (Cell Signalling), mouse monoclonal anti-polyQ 1C2 (Trottier et al., 1995), mouse monoclonal anti-ataxin-7 1C1 (Yvert et al., 2000), mouse monoclonal anti-rhodopsin 4D2 (gift from D. Hicks) and mouse monoclonal anti-β-tubulin (Chemicon), were used at 1:1000 dilutions and revealed with appropriate anti-mouse or anti-rabbit peroxidase-conjugated secondary antibodies (Jackson ImmunoResearch Laboratories) and the ECL chemiluminescent reaction (Pierce).

Plasmid constructs

Site-directed mutagenesis was performed to create the JunAA mutant in pcDNA3.1, and the coding region of the JunAA construct was sequenced to establish that no additional changes had been introduced. The primers used for the mutagenesis were S63Afor 5′ ctcggacctcctcaccgcgcccgacgtggggctgc-3′, S63Arev 5′-gcagccccacgtcgggcgcggtgaggaggtccgag-3′, S73Afor 5′-ggctgctcaagctggcggcgcccgagctggagcgcc-3′, and S73Arev 5′-ggcgctccagctcgggcgccgccagcttgagcagcc-3′. Gene fragments of 2.4 kb (Nl) from the 5′ flanking region of the mouse Nrl promoter were amplified and cloned into pGL3-basic vector (Madison, WI) in-frame with the luciferase reporter gene. Site-directed mutants of the mouse Nrl promoter, pGL3-Nl-mAP1A (removes TGATCTCA at position −50 to −43) and pGL3-Nl-mAP1B (removes TCATCTTATTGGA at position −83 to −71) were generated from pGL3Nl using the QuickChange site-directed mutagenesis kit (Stratagene) and were sequence-verified. Primers used to generate the mutant Nrl promoter constructs are: mAP1AFor 5′-gctcgaggaccacagagggaaccagtccttta-3′, mAP1ARev 5′-taaaggactggttccctctgtggtcctcgagc-3′, mAP1BFor 5′-aR7Ecaaataagcccttgaggctcgaggac-3′, and mAP1BRev 5′-gtcctcgagcctcaagggcttatttgcat-3′.

Luciferase assays

The reporter activity assays were performed by the published method (Bessant et al., 1999) with minor alterations. Briefly, human embryonic kidney 293 (HEK-293) cells (from American Type Culture Collection, CRL-1573) were seeded at 4×10^4 cells per well in 24-well plates and 0.33 μg of Jun or JunAA were transfected with pGL3-Nl-mAP1B. Empty pcDNA4 vector and cytomegalovirus-beta-galactosidase vector were included to control for the amount of transfected DNA and transfection efficiency, respectively. Transfections were performed using FuGENE 6 (Roche Diagnostics). Cells were harvested after 48 hours. Luciferase assays (Luciferase Assay System, Promega) were repeated in triplicate three times and calculated as a fold change from the baseline (empty pcDNA4 expression vector).

Footprinting

Bovine retinal nuclear extract (RNE) was prepared as described (Lahiri and Ge, 2000), except that 400 mM KCl was used instead of NaCl. Solid phase DNase I footprinting (Sandaltzopoulos and Becker, 1994) was performed using 100 mg RNE. Nrl-l-EGFP plasmid was used as template for region I. A sequencing reaction was loaded on the gel next to the footprinting reactions to identify the exact location of footprints. Results were analyzed by Transcription Element Search System (http://www.cbil.upenn.edu/tess/) and Alibaba2 (http://www.alibaba2.com/).

Results

C-Jun phosphorylation modulates rod photoreceptor activity

The R7E mice over-express full-length ataxin-7 with 90 Q in rods and exhibit a progressive retinopathy, which is characterized by an early functional and morphological alteration of rod cells (Yvert et al., 2000). To investigate the role of JNK/c-Jun stress signaling pathway, the R7E mice were bred to JunAA knock-in mice, in which JNK-mediated activation of c-Jun is compromised, through Alanine replacement of Serine 63 and 73. In contrast to the Jun knock-out mice, which are embryonic lethal, JunAA mice are healthy, fertile and resistant to excitotoxic stress (Behrens et al., 1999). As predicted, JNK-mediated phosphorylation of c-Jun is abolished in JunAA-R7E transgenic mice (JunAA-R7E) (Fig. 1a). To evaluate the functional effect of c-Jun phosphorylation on SCA7 retinopathy, we recorded the rod electroretinograms (ERGs) for R7E, *Junaa/wt*-R7E, *Junaa/aa*-R7E, wild-type, *Junaa/wt* and *Junaa/aa* mice, at 3 months of age when rod dysfunction is prominent (Fig. 1b). R7E and *Junaa/wt*-R7E mice exhibited similarly altered rod activity, but the rod response of *Junaa/aa*-R7E (JunAA-R7E) mice was improved. The rod function of *Junaa/aa* mice (JunAA) was also increased, when compared to that of wild-type and *Junaa/wt* animals. We therefore pooled the R7E and *Junaa/wt*-R7E animals, whose rod activities were not statistically different, and referred to them as CT-R7E. Similarly, the control animals (called CT) included both wild-type and *Junaa/wt* mice, which also show no difference at the histological level (not shown). At 3 months, a-wave amplitude of CT-R7E mice was reduced by 65% when compared to CT animals while it was lower by 40% in JunAA-R7E mice, and the rod response of JunAA mice was increased by 17% when compared to CT mice (Fig. 1c). Thus, the function of rod photoreceptors seems to have improved when amino-terminal phosphorylation of c-Jun is abolished.

The JunAA mutation slows down segment flattening by polyQ-ataxin-7

Histologically, in agreement with a previous report (Grimm et al., 2001), retinas of JunAA mice were indistinguishable from CT retinas (Fig. 2, and data not shown). The number and composition (cone/rod ratio) of photoreceptors was comparable in two groups, as revealed with lectin PNA, which specifically labels cone-associated matrix (Fig. 2a). However, a few differences were apparent between JunAA-R7E and CT-R7E retinas at 3 months. Rod dysfunction in R7E mice is characterized by progressive disorganization of photoreceptors, including the outer nuclear layer (ONL), which acquires a “wavy” shape, and segments whose thickness is dramatically reduced (Yvert et al., 2000; Helmlinger et al., 2002). NIs, which contain aggregated and cleaved polyQ-ataxin-7, progressively appear throughout the ONL (Yvert et al., 2000). Immunofluorescence studies revealed that, although the “wavy” shape and NIs of the ONL remained prominent, the thickness of the segments as stained with an anti-rhodopsin antibody appeared less

reduced in JunAA-R7E than in CT-R7E mice at 3 months (Fig. 2b). This suggested that at 3 months, the JunAA mutation slows down the pathological process. At early stages of R7E pathology (i.e., up to 6 months of age), histological analyses revealed no significant reduction of the ONL, and no obvious signs of cell death were evident ((Helmlinger et al., 2004b) and data not shown), indicating that c-Jun phosphorylation modulates rod photoreceptor activity rather than survival.

Expression levels of Nrl and its target genes are enhanced when c-Jun phosphorylation is compromised

Rod photoreceptor activity is controlled by specific transcription factors, including Nrl and Crx (Rehemtulla et al., 1996; Chen et al., 1997; Furukawa et al., 1999; Mears et al., 2001). We asked whether the expression of these transcription factors is enhanced in the absence of c-Jun phosphorylation. Quantitative real-time PCR using retinal RNA from JunAA and CT mice showed that *Nrl* expression was increased by 2-fold in JunAA mice (Fig. 3a). Western-blotting experiments using retinal extracts validated *Nrl* upregulation at the protein level (Fig. 3c). In contrast, the expression of *Crx* was unaltered (Fig. 3a). Nrl is essential for the optimal expression of various rod phototransduction genes, including *Rho*, *Gnat1* and *Pdeb* (Mears et al., 2001; Yoshida et al., 2004); expression of these genes was augmented in JunAA mice (Fig. 3a). Consistently, Rho protein was also increased in JunAA mice (Fig. 3d). In contrast, the expression of rhodopsin kinase, which does not appear to be regulated by Nrl, did not reveal any change. We confirmed that *Nrl* expression was strongly downregulated in transgenic retinas, reaching 20% of the control expression (Fig. 3b, and (Abou-Sleymane et al., 2006)). *Crx* expression was also reduced though to a lesser extent (Fig. 3b). As a consequence, the expression of *Rho*, *Gnat1* and *Pdeb* were dramatically impaired (Fig. 3b). In R7E animals, the JunAA mutation led to a significant increase of Nrl, both at the level of mRNA and protein, while it did not modify *Crx* mRNA expression (Figs. 3b and c). Expression of *Pdeb* was significantly increased in JunAA-R7E mice, and that of *Rho* and *Gnat1* showed a tendency to increase (Figs. 3b and d).

Results from knock-out studies have shown that *Nrl* and *Crx* are both required for *Rho* and *Gnat1* expression (Furukawa et al., 1999; Mears et al., 2001). Indeed, in the absence of one or the other, expressions of *Rho* and *Gnat1* are negligible. Notably, Nrl is required for *Pdeb* expression, while Crx is not (Furukawa et al., 1999; Lerner et al., 2001; Mears et al., 2001). Since in JunAA-R7E mice *Crx* expression is as impaired as in CT-R7E mice, we hypothesized that *Nrl* primarily promotes *Pdeb* expression in our context. Our results thus showed that amino-terminal phosphorylation of c-Jun repressed expression of *Nrl* transcripts. By preventing c-Jun phosphorylation of R7E mice, the expression of *Nrl* and its downstream effector *Pdeb* could be partially restored, thereby providing a molecular mechanism for functional improvement of rod photoreceptor function in JunAA-R7E mice.

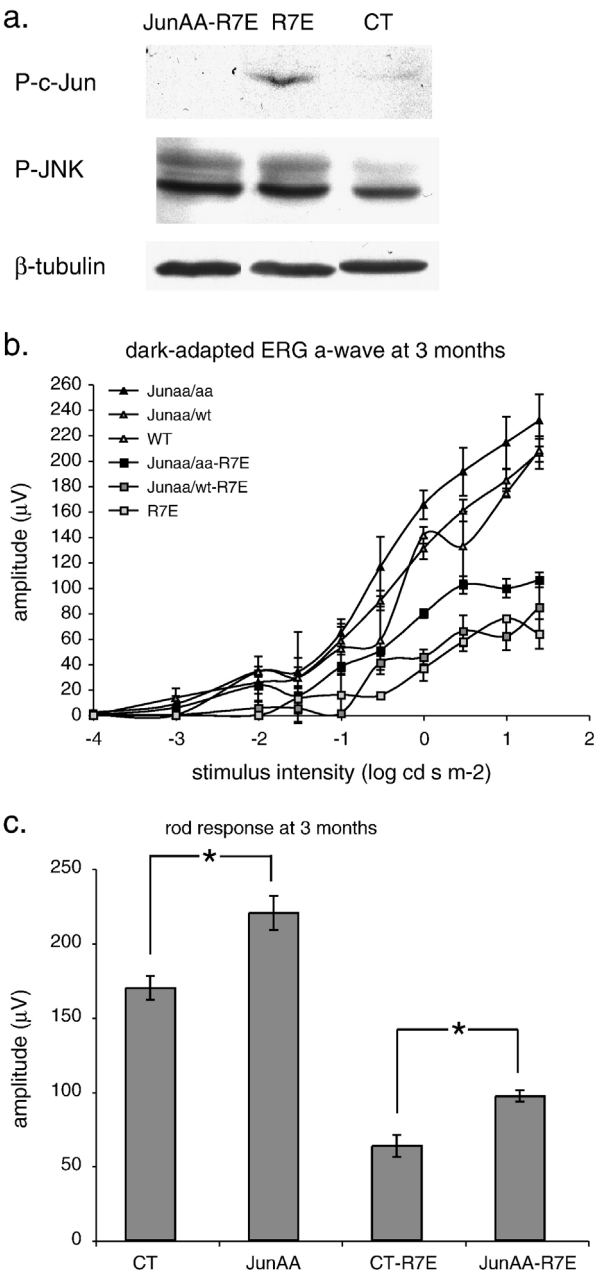

Fig. 1. c-Jun phosphorylation modulates rod photoreceptor activity. (a) JNK-mediated phosphorylation of c-Jun is abolished in SCA7 transgenic mice expressing mutated c-Jun. Western-blotting analysis of whole cell protein extracts from 3 month old retinas of JunAA transgenic (JunAA-R7E), R7E and control (CT) animals, using anti-phospho-cJun and anti-phospho-JNK antibodies. Antibody against β-tubulin was used as a loading control. (b) The JunAA mutation induces an increase in rod photoreceptor activity. Intensity-response curves of the dark-adapted ERG a-wave at 3 months of age for three R7E mice, 5 R7E mice heterozygous for the JunAA mutation (Junaa/wt-R7E), 6 R7E mice homozygous for the JunAA mutation (Junaa/aa-R7E), three wild-type mice (WT), 10 mice heterozygous for the JunAA mutation (Junaa/wt) and 8 mice homozygous for the JunAA mutation (Junaa/aa). (c) Comparison of the rod response between JunAA-R7E (Junaa/aa-R7E) and CT-R7E (Junaa/wt-R7E and R7E were pooled to constitute the CT-R7E group), and between JunAA (Junaa/aa) and CT (Junaa/wt and WT were pooled) at 3 months of age. Junaa/wt-R7E and R7E, as well as Junaa/wt and WT animals were not statistically different. Each bar represents the amplitude value calculated by averaging the last 4 dark-adapted ERG amplitudes measured at maximum light intensities and represented on panel b (JunAA-R7E: 96.99 μv +/−3.84 μv, $n=6$; CT-R7E: 63.59 μv+/−7.32, $n=8$; JunAA: 201.00 μv+/−16.15, $n=8$; CT: 169.75 μv+/−8.22, $n=13$). Statistical analyses were performed using Kruskal-Wallis test followed by Wilcoxon test for post-hoc comparisons; *, $p<0.05$.

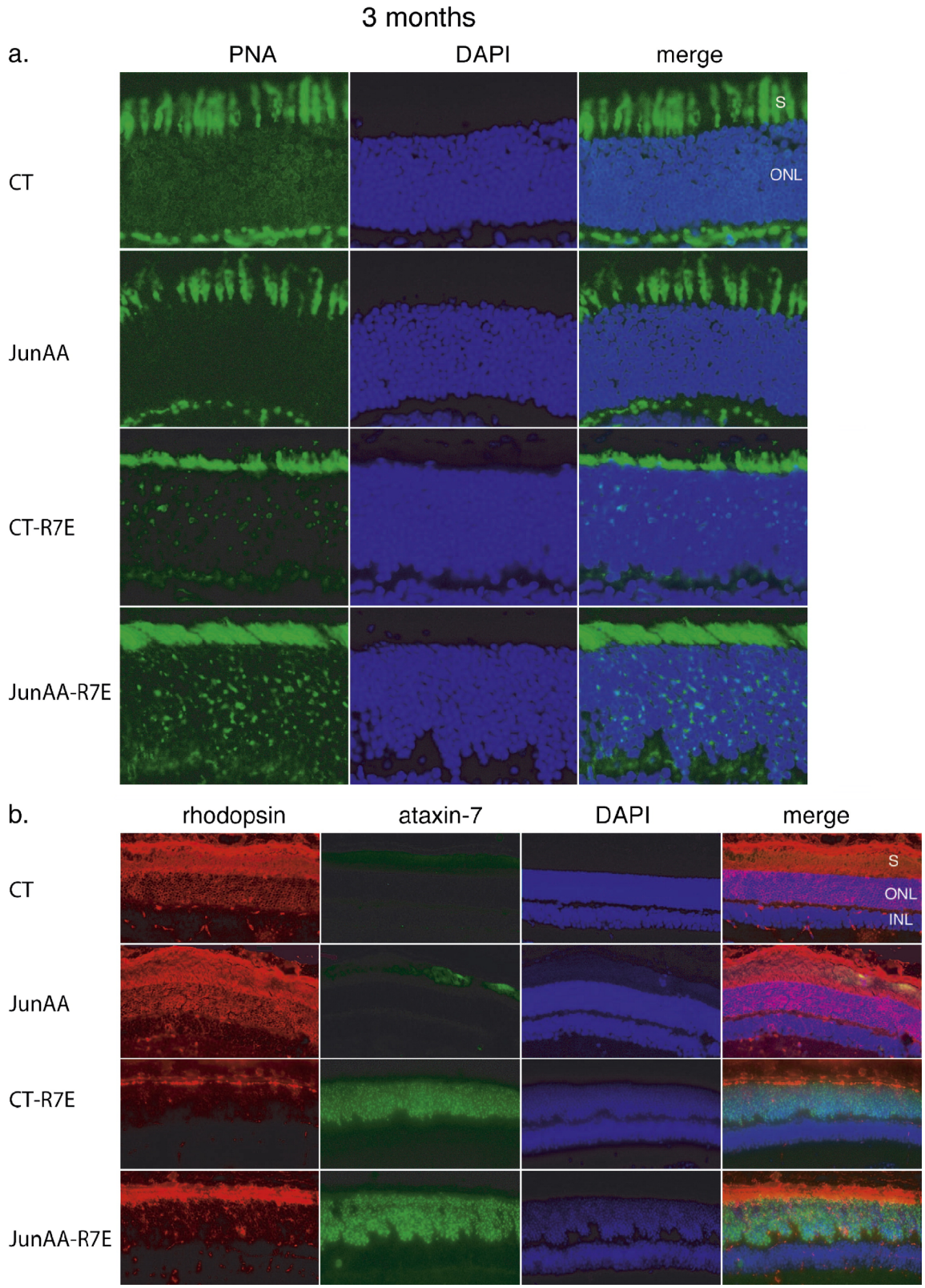

Fig. 2. The JunAA mutation slows thinning of photoreceptor segments in R7E animals. Immunofluorescence microscopy of retinal cryosections of JunAA-R7E, CT-R7E, JunAA and CT mice. (a) Sections were stained with the lectin PNA. (b) sections were double stained with anti-rhodopsin antibody (red) and anti-ataxin-7 antibody (green). Nuclei are revealed with DAPI. S, segments; ONL, outer nuclear layer; INL, inner nuclear layer. Thickness of the segments had a tendency to be less reduced in JunAA-R7E than in CT-R7E mice ($p=0.08$), and no obvious difference was observed between JunAA and CT mice (JunAA-R7E: 21.45 μm+/−4.50, $n=3$; CT-R7E: 14.97 μm+/−3.66, $n=3$; CT: 30.63 μm+/−2.12, $n=4$; JunAA: 32.85 μm+/−5.51, $n=4$). Statistical analyses were performed using Kruskal-Wallis test followed by Wilcoxon test for post-hoc comparisons.

PolyQ-ataxin-7 transgene expression is upregulated in JunAA-R7E mice

To evaluate whether the partial rescue observed in JunAA-R7E mice may be the consequence of decreased transgene expression, we compared polyQ-ataxin-7 expression levels of JunAA-R7E and CT-R7E mice. Quantitative real-time PCR showed that transgene expression was significantly upregulated in JunAA-R7E mice (Fig. 4a). Expression of polyQ-ataxin-7 is under the control of the rhodopsin promoter in SCA7 transgenic mice. The JunAA mutation had a minor effect on *Rho* expression (Fig. 3b), suggesting that activities of endogenous and transgene rhodopsin promoters are modulated by their respective chromatin environments. In R7E mice, NIs formation is associated with progressive cleavage of polyQ-ataxin-7 protein (Yvert et al., 2000; Helmlinger et al., 2004a). By fractionation and western-blotting experiments, a cleaved product of about 37 kDa was revealed with both the 1C1, an anti-ataxin-7 antibody raised against the N-terminus part of ataxin-7, and the 1C2 antibody, which preferentially reveals extended polyQ (Supplementary Fig. a). Over time, polyQ-ataxin-7 is primarily composed of this cleaved, aggregated and insoluble fragment ((Yvert et al., 2000) and data not shown). Western-blotting analyses of insoluble protein fractions confirmed that increased amounts of polyQ-ataxin-7 accumulated in 3-month old JunAA-R7E mice, compared to CT-R7E animals (Fig. 4b). This may finally lead to enhanced toxicity in JunAA-R7E animals. Indeed, at 4.5 months, the expression of *Nrl* and *Pdeb* was similar in JunAA-R7E and CT-R7E mice (Fig. 4c) and the rod activity was comparable in JunAA-R7E and CT-R7E mice, although at that age it was increased in JunAA mice when compared to the control animals (Fig. 4d). At 4.5 months, the expression of the transgene was also similar between JunAA-R7E and CT-R7E animals, although polyQ-ataxin-7 protein remained more abundant in JunAA-R7E mice (Supplementary Figs. b and c), indicating that degradation of mutant protein is a slow process. Our data provided evidence that increased accumulation of polyQ-ataxin-7 in JunAA-R7E mice induces a secondary level of toxicity, which eventually prevents the benefit of the JunAA mutation. This secondary effect should be however considered as a model artifact, probably caused by an Nrl-dependent promoter.

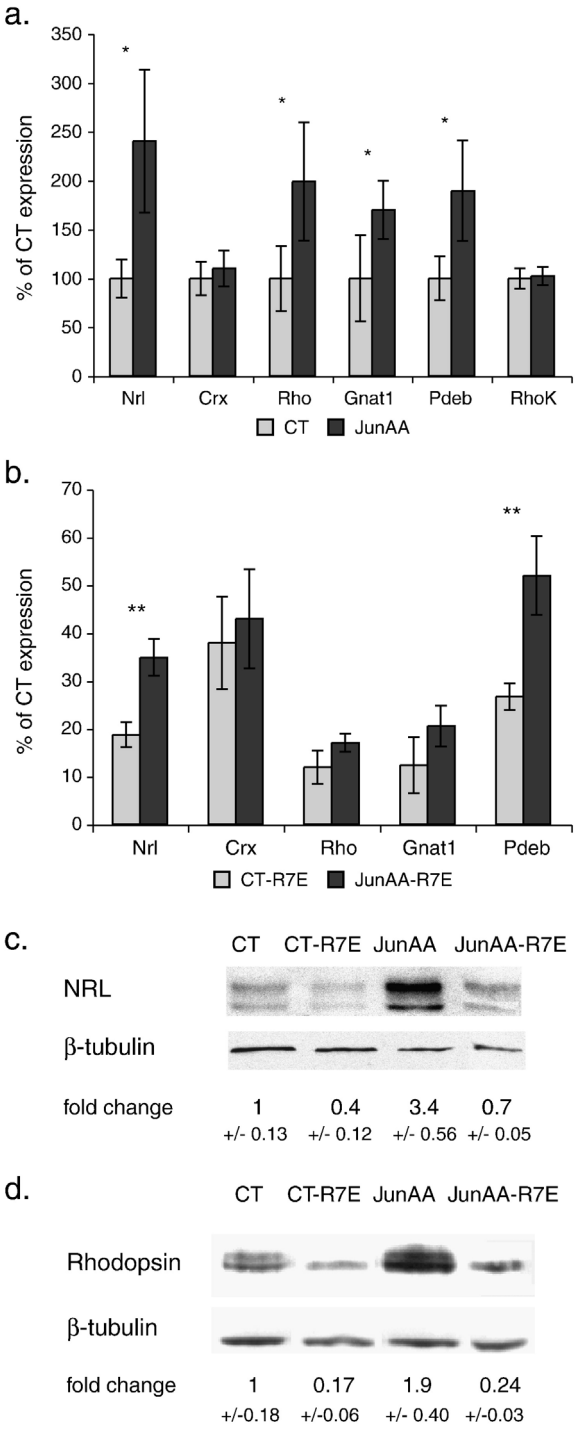

C-Jun can directly regulate Nrl expression

We then asked whether c-Jun/AP-1 could directly regulate *Nrl* expression. To address this, footprinting experiments were

Fig. 3. c-Jun phosphorylation contributes to the regulation of Nrl expression. (a) Real-time RT-PCR analysis of total RNA extracted from adult (4.5 months) JunAA and CT retinas, using primers specific for Nrl, Crx, Rho, Gnat1, Pdeb and RhoK. Primers amplifying 36B4 or cyclophilin were used as internal controls. JunAA mRNA levels are quantified as a percentage of CT mRNA, after normalization to internal control level. Each bar represents the mean value+/−SEM (JunAA: $n=3$; CT: $n=5$). Nrl, Rho, Gnat1 and Pdeb expressions were significantly increased in JunAA mice. Stastistical analysis was performed using a Student's *t*-test. *, $p<0.05$. Similar results were obtained at 3 months (not shown). (b) Real-time RT-PCR analysis of total RNA extracted from 3 month JunAA-R7E and CT-R7E retinas. JunAA-R7E and CT-R7E mRNA levels were expressed as a percentage of CT mRNA, after normalization to internal control level (JunAA-R7E: $n=7$; CT-R7E: $n=5$, CT: $n=2$). Nrl and Pdeb expressions were significantly increased in JunAA-R7E mice, compared to CT-R7E. **, $p<0.01$, Student's *t*-test. (c and d) Western-blotting analysis of whole cell protein extracts from 3 month JunAA-R7E, CT-R7E, JunAA and CT retinas, using anti-Nrl antibody (c) and anti-rhodopsin antibody (d). Anti-β-tubulin antibody was used as control. The anti-Nrl antibody detected multiple bands, the upper bands corresponding to phosphorylated forms of Nrl. Fold-change of Nrl and Rho levels were calculated from 3 to 6 retinas for each mouse genotype. Nrl and Rho are increased in JunAA, when compared to CT mice ($p<0.001$ and $p<0.05$, respectively). Nrl is also increased in JunAA-R7E, when compared to CT-R7E mice ($p<0.05$), while Rho is not statistically different between JunAA-R7E and CT-R7E mice ($p=0.16$). Statistical analyses were performed using Kruskal-Wallis test followed by Wilcoxon test for post-hoc comparisons.

performed using the proximal promoter region of *Nrl* (Fig. 5a). We show that this region upstream of the Nrl transcription start site contains one AP-1/CRE site (TGATCTCA) proximal to the TATA-box of the gene (Farjo et al., 1997) and a second that overlaps a Ret1/PCEI element (Fig. 5b). To investigate the role of these putative AP-1 elements in c-Jun-mediated inhibition of Nrl, we measured the luciferase activity in HEK-293 cells transfected with constructs containing the entire promoter of Nrl (Fig. 5c, and data not shown). Co-transfection with c-Jun modestly but reproducibly decreased the expression of the reporter luciferase gene. A similar result was obtained when the first AP-1-like/CRE element was removed from the promoter (data not shown). On the other hand, transcriptional activity experiments with reporter constructs carrying a deletion in the Ret1/PCEI/AP1 region indicated that c-Jun repression may be mediated through this site (Fig. 5c).

Amino-terminal phosphorylation of c-Jun stimulates transactivation but not DNA binding (Karin, 1995). In SCA7 transgenic mice, the increase of amino-terminal phosphorylation of c-Jun correlated with increased expression of c-Jun, both at the protein and the mRNA level (Fig. 5d and data not shown), likely because c-Jun is autoregulated (Angel et al., 1988). Conversely, the JunAA mutation resulted in decreased expression of c-Jun (Fig. 5d). We suggest that activation of c-Jun by polyQ-ataxin-7 induces c-Jun expression, which in turn promotes the binding of c-Jun to the Nrl promoter thereby repressing the expression of *Nrl*. In agreement with this hypothesis, the luciferase activity generated from the *Nrl* promoter is equally altered by overexpression of c-Jun or by the unphosphorylatable version of c-Jun (cJunAA) (Fig. 5c). The AP-1 site identified here overlaps with a Ret1/PCEI site, which is present in several retinal genes (Farjo et al., 1997; Mathers et al., 1997), indicating that binding of c-Jun/AP-1 to *Nrl* promoter may compete with the binding of the protein bound to this site, thus preventing maximal transcription.

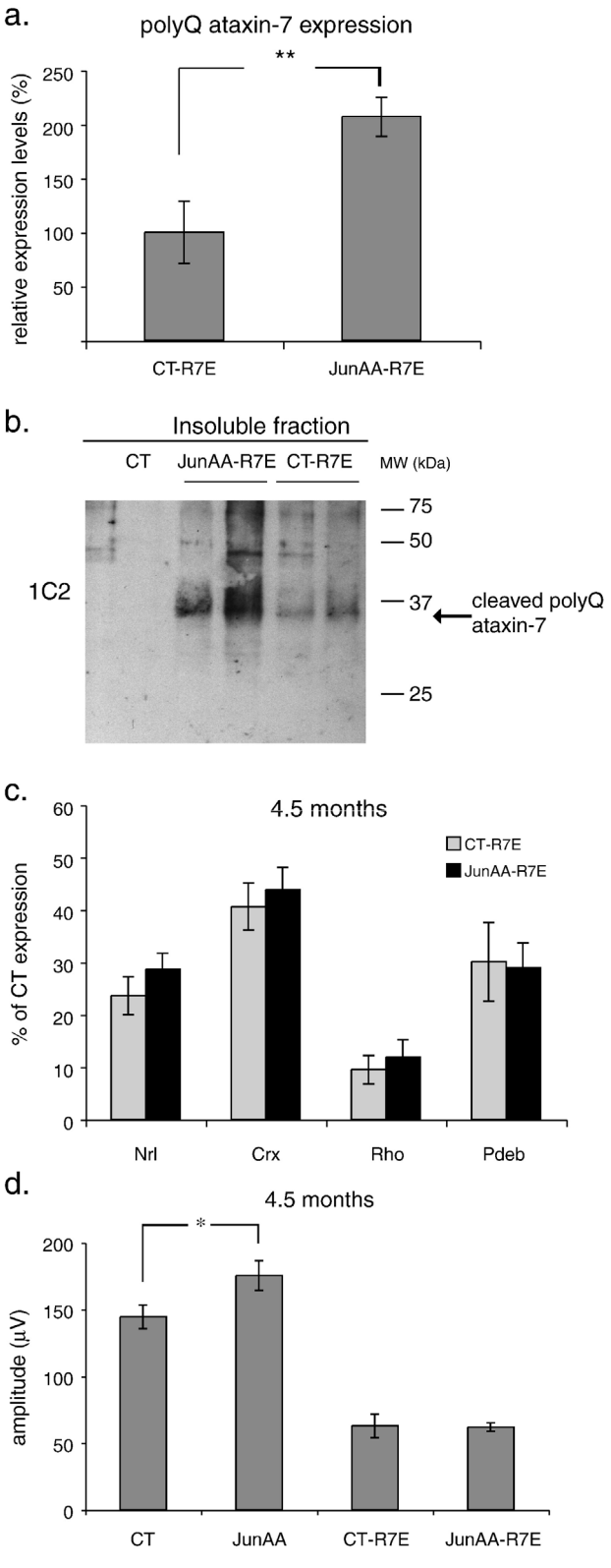

Fig. 4. PolyQ-ataxin-7 expression, which is regulated by an Nrl-dependent promoter, is upregulated in JunAA-R7E mice. (a) Real-time RT-PCR analysis of total RNA extracted from 3 month JunAA-R7E and CT-R7E animals, using primers specific for recombinant SCA7 and 36B4, as an internal control. JunAA-R7E SCA7 mRNA level was quantified as a percentage of CT-R7E mRNA level. PolyQ-ataxin-7 expression was two-fold increased in JunAA-R7E mice (JunAA-R7E: $n=7$; CT-R7E: $n=5$; *, $p<0.01$, Student's *t*-test). (b) Western-blotting analysis of insoluble fractions prepared from 3 month CT, JunAA-R7E and CT-R7E retinas, using the 1C2 antibody which detects polyQ. PolyQ-ataxin-7 accumulated as a cleaved insoluble fragment. Accumulation of polyQ-ataxin-7 was more prominent in JunAA-R7E than in CT-R7E animals. (c) Real-time RT-PCR analysis of total RNA extracted from 4.5 month JunAA-R7E and CT-R7E animals, using primers specific for Nrl, Crx, Rho, Pdeb and 36B4, as an internal control. JunAA-R7E and CT-R7E mRNA levels were expressed as a percentage of CT level (JunAA-R7E: $n=4$; CT-R7E: $n=5$; CT: $n=2$). Expressions of Nrl, Crx, Rho and Pdeb were not different in JunAA-R7E and CT-R7E animals. (d) Analysis of the rod response of JunAA, CT, JunAA-R7E and CT-R7E animals at 4.5 months (JunAA: 175.42 µv+/−11.11, $n=6$; CT: 144.52 µv+/−8,93, $n=11$, including 7 Junaa/wt and 4 WT, JunAA-R7E: 62.05 µv+/−3.11, $n=7$; CT-R7E: 62.91 µv +/−8.83, $n=10$, including 7 Junaa/wt-R7E and 3 R7E; *, $p<0,05$, Kruskal-Wallis followed by Wilcoxon test).

Discussion

Deciphering pathophysiological mechanisms implicated in polyQ expansion disorders is an important step towards better design of therapeutics. To address the *in vivo* relevance of JNK/c-Jun stress pathway in polyQ toxicity, we investigated the genetic interaction between c-Jun phosphorylation and polyQ-ataxin-7 in the mouse retina. We used a transgenic mouse model of SCA7 that restricts polyQ-ataxin-7 expression to rod photoreceptors. This model recapitulates rod dystrophy observed in SCA7 patients.

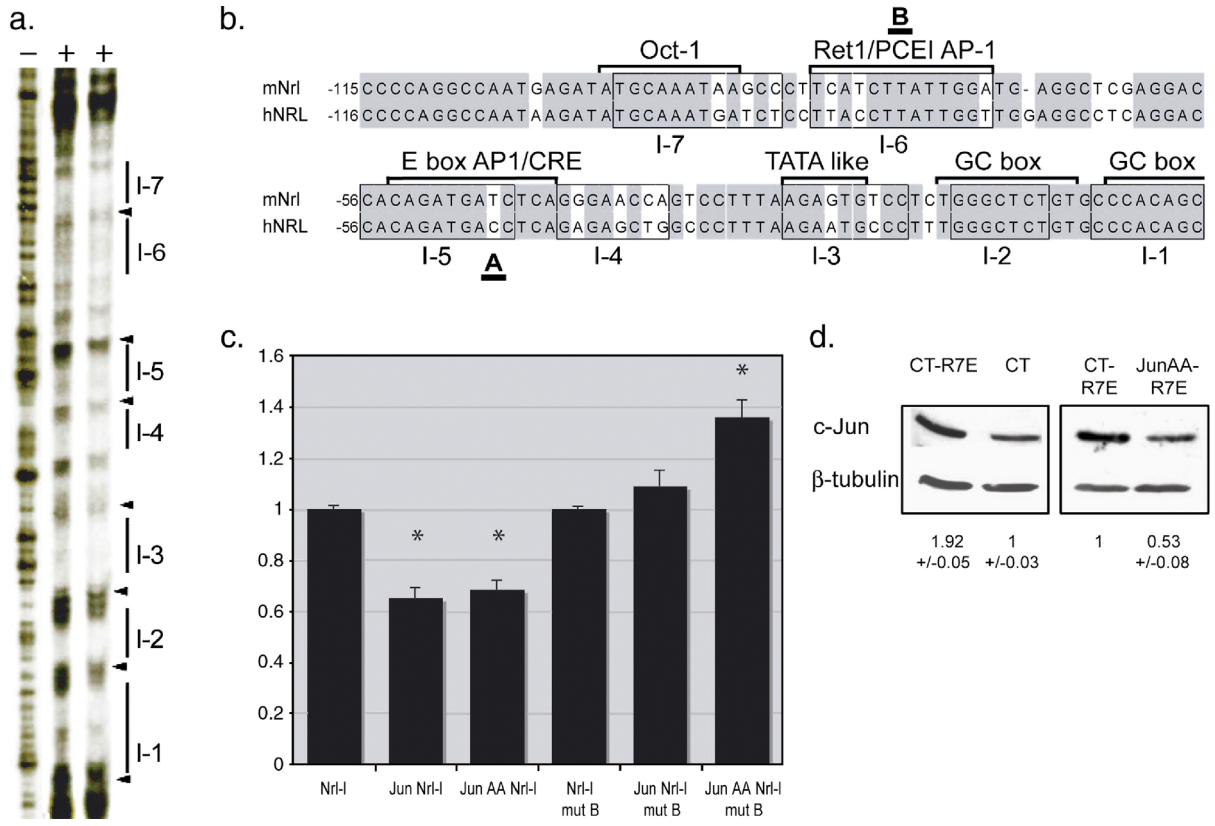

Fig. 5. DNase footprinting and reporter assays of the Nrl promoter. (a) DNase I footprinting of the proximal mouse Nrl promoter using bovine retinal nuclear extract. Footprints are marked by lines and numbered I-1 through I-7. (−), no RNE; (+) with RNE. The footprints corresponding to the EboxAP1/CRE site and the Ret1/PCEI AP-1 site are I-5 and I-6 respectively. (b) DNA sequences of the proximal mouse Nrl promoter. Boxed regions indicate DNase footprints and brackets show presumed binding sites for transcription factors. The location of the putative AP1 sites TGATCTCA and TCATCTTATTGGA are denoted by the letters 'A' and 'B', respectively. (c) Luciferase experiments testing the effect of Jun or JunAA on wildtype (Nrl-l) and mutant (Nrl-l-mAP1B) promoter. Nrl-l-mAP1B lacks the putative AP1 site TCATCTTATTGGA. Addition of Jun (Jun Nrl-l) or JunAA (JunAA Nrl-l) slightly decreased luciferase activity of the Nrl promoter. Mutation of the putative AP1 site eliminated the repressive effect of Jun (Jun Nrl-l mutB) and JunAA (JunAA Nrl-l mutB). Activities that are statistically different from controls (Student's *t*-test, $p<0.001$) are marked with an asterisk. (d) Western-blotting analysis of whole cell protein extracts from 3 month JunAA-R7E, CT-R7E and CT retinas, using anti-c-Jun antibody. The anti-β-tubulin antibody was used as loading control. C-Jun protein is increased in SCA7 transgenics, compared to wild-type mice, and the JunAA mutation results in decreased levels of c-Jun protein in retinas of SCA7 animals. Fold-change of c-Jun levels were calculated from 2 to 3 retinas for each mouse genotype.

Interestingly, the Huntington's disease (HD) transgenic R6/2 mouse model, in which expression of a polyQ fragment of the HD protein – huntingtin– is under the control of its own promoter, also displays a retinopathy comparable to that observed in retinal SCA7 mice, at physiological, morphological and molecular levels (Helmlinger et al., 2002; Abou-Sleymane et al., 2006). Although the retina is not affected in HD patients, these observations support the hypothesis that the retina represents a valuable paradigm to decipher molecular mechanism(s) implicated in polyQ-induced toxicity. Here we show that improvement of rod function in JunAA-R7E mice correlates with upregulation of *Nrl* and its target gene *Pdeb*, which is a critical regulator of phototransduction, We further show that c-Jun can directly repress *Nrl*, thus providing a mechanistic clue to the beneficial effect of c-Jun phosphorylation inhibition on SCA7 retinopathy.

Over time, the expression of *Rho* and the transgene, which is under the control of the *Rho* promoter (a target of Nrl), are both downregulated in R7E mice (Helmlinger et al., 2004b and Supplementary Fig. d). Conversely, expressions of *Nrl*, *Pdeb* and the transgene are increased in 3-month old JunAA-R7E retinas. Increasing concentration and incubation duration of polyQ proteins or peptides result in more cellular toxicity (Yang et al., 2002). Thus, we suggest that the mechanism contributing to the correction of the molecular defects–increased expression of *Nrl*–also promotes toxicity, through increasing the expression of polyQ-ataxin-7. Our data (Fig. 4 and Supplementary Fig.) suggest that the beneficial effect of the JunAA mutation on *Nrl* expression might finally be prevented by the deleterious effect resulting from increased polyQ-ataxin-7 protein. The balance between the two opposing effects might actually determine the outcome. PolyQ-ataxin-7 protein remains more abundant in JunAA-R7E than in CT-R7E mice at 4.5 months, as shown in the Supplementary Figure. We propose that the slow turnover of the highly prone to aggregation polyQ-ataxin-7 protein is responsible for the increased accumulation of polyQ-ataxin-7 protein in the 4.5-month old JunAA-R7E mice, which might finally favor the artifact toxic effect of the JunAA mutation.

Modelling of SCA7 disease in the mouse using either transgenic or knock-in approaches leads to impairment of various rod phototransduction genes, including *Rho*, *Gnat1* and *Pdeb* (Yoo et al., 2003; Helmlinger et al., 2004b; Abou-Sleymane et al., 2006). Expressions of *Nrl* and *Crx*, which are primary transcriptional regulators of phototransduction genes, are decreased by 5- and 2.5-

fold, respectively, in R7E mice (Fig. 3b, and (Abou-Sleymane et al., 2006)). Interestingly, Nrl and Crx are known to co-regulate *Rho* and *Gnat1* (Chen et al., 1997), suggesting that downregulation of *Nrl* or *Crx* may compromise the expression of both *Rho* and *Gnat1*, which are reduced by 10-fold in R7E mice (Fig. 3b). In contrast, we find that the expression of *Pdeb* is decreased by 4-fold. Previous studies have shown that Nrl but not Crx is required for *Pdeb* expression (Furukawa et al., 1999; Mears et al., 2001), indicating that downregulation of *Pdeb* directly correlates to the downregulation of *Nrl*. Consistent with this hypothesis, a 2-fold upregulation of *Nrl* in the JunAA mouse background correlates with a 2-fold upregulation of *Pdeb*, whereas expressions of *Rho* and *Gnat1* are less enhanced. As Pdeb is a critical rate-limiting enzyme in phototransduction, we propose that upregulation of *Nrl* causes upregulation of *Pdeb*, which contributes to amelioration of rod function in 3-month old JunAA-R7E mice.

In humans, loss of function mutations in the *NRL* gene leads to severe rod photoreceptor dystrophy, while blue cone function is preserved (Nishiguchi et al., 2004). The $Nrl^{-/-}$ mice present a similar phenotype, characterized by complete loss of rod function and super-normal cone function (Mears et al., 2001). Rod photoreceptor function is also impaired in SCA7 patients and in mouse models. However, SCA7 patients suffer from a cone-rod dystrophy. SCA7 knock-in mice and transgenic mice expressing polyQ-ataxin-7 controlled by prion promoter recapitulate degeneration of both cone and rod photoreceptors (La Spada et al., 2001; Yoo et al., 2003). In addition, cone function of R7E transgenic mice is impaired, although to a lesser extent than rod function, as revealed by ERGs (data not shown). Lastly, expression of a number of cone genes, including blue and green cone opsins is decreased in R7E mice (Abou-Sleymane et al., 2006). *Crx*, which is reduced in R7E mice, acts as a critical regulator of both cone and rod photoreceptor genes. Its transcriptional activity was decreased in another SCA7 transgenic mouse model (Chen et al., 2004b), although it was not impaired in the SCA7 knock-in mice (Yoo et al., 2003). Thus, altered *Crx* expression may contribute to functional changes in both rod and cone photoreceptors in SCA7 disease. DNA microarray analyses revealed that *Nr2e3*, *ErrB* and *Mef2C* were also deregulated in R7E mice (Abou-Sleymane et al., 2006), indicating that a network of transcriptional regulators involved in photoreceptor function and fate are likely impaired in SCA7 retinopathy.

JNK/c-Jun pathway is activated in response to various stresses and controls both cell life and death programs (Shaulian and Karin, 2001). Mice deficient for JNK3, the brain specific isoform of JNK, are normal but resistant to neuronal death caused by excitotoxic stress (Yang et al., 1997). Indeed, kainate-treated hippocampal neurons of *Jnk3*−/− mice are protected against cell death. Interestingly, JunAA mice display a similar phenotype (Behrens et al., 1999), indicating that JNK/c-Jun-mediated neuronal degeneration requires transcriptional-dependent processes. We show here that the R7E phenotype is modulated by the JunAA mutation, suggesting that polyQ-ataxin-7-induced activation of JNK/c-Jun pathway is a component of the pathological process. At 3 months, the R7E phenotype is improved by mutations in c-Jun phosphorylation sites. Interestingly, at that age, photoreceptor dysfuntion is prominent but death is not evidenced (Helmlinger et al., 2004b). Thus, our data implicate that polyQ-ataxin-7-induced activation of AP-1 promotes photoreceptor dysfunction rather than death. We had shown that the JNK/c-Jun pathway was persistently but moderately activated in R7E retinas (Merienne et al., 2003). The transcriptional effects induced by moderate activation of c-Jun might differ from those obtained by kainate, which induces robust activation of c-Jun and leads to rapid neuronal death. Alternatively, the function of c-Jun/AP-1 might be different between hippocampal neurons and retinal photoreceptors.

We show here that c-Jun can directly inhibit expression of *Nrl*, which is required for rod function. Interestingly, repression of AP-1 dependent target genes has been proposed to account for light-induced apoptosis of photoreceptors (Grimm et al., 2001; Wenzel et al., 2002). Indeed, despite its lack of transactivation domains, Fra-1 can substitute for c-Fos in light-induced photoreceptor apoptosis, suggesting that AP-1, which usually activates genes, acts as a suppressor of anti-apoptotic or survival photoreceptor genes (Wenzel et al., 2002). AP-1 has further been shown to negatively regulate specific genes. For instance, binding of c-Jun to the AP-1 element within the *mdr-1* promoter results in repression of *mdr-1*, a gene activated in certain multi-drug resistance (MDR) tumor cells (Miao and Ding, 2003; Chen et al., 2004a). In MDR cells, treatment with salvicine induces activation of JNK and c-Jun, enhancement of *c-jun* expression and its DNA binding activity, and finally repression of *mdr-1*. The series of events we describe in R7E mice, leading to c-Jun-mediated *Nrl* repression, appear to be very similar. Furthermore, c-Jun/AP-1 has been shown to repress expression of tissue-specific genes, including osteocalcin, a bone-specific marker and the pituitary-specific transcription factor (Pit-1/GHF-1) (Owen et al., 1990; Delhase et al., 1996). Interestingly, in both cases, the repression mechanism involves a mutually exclusive occupancy of AP-1 and tissue-specific transcription factors. Similarly, we show that c-Jun/AP-1 inhibits expression of the rod-specific gene *Nrl* through an AP-1 site overlapping a tissue-specific Ret1-PCEI element (Mathers et al., 1997).

DNA microarray analyses performed on R7E retinas have suggested that polyQ-ataxin-7 induces a global cellular response resulting in dysfunction through alteration of photoreceptor differentiation program (Abou-Sleymane et al., 2006). Interestingly, Stat3 transcription factor, which inhibits photoreceptor differentiation through downregulation of *Crx* expression (Ozawa et al., 2004; Zhang et al., 2005), was overexpressed and hyperphosphorylated in R7E mice. Like c-Jun, Stat3 is a sensor of cellular stress, suggesting that stress-induced activation of c-Jun and Stat3 by polyQ-ataxin-7 might converge to alteration of photoreceptor fate and function, via downregulation of primarily *Nrl* and probably *Crx*.

Acknowledgments

We thank J.L. Mandel, F. Klein and M. Ravache for discussions, E. Metzger and staff at the IGBMC animal facility for mouse care, J-.L-. Vonesh and D. Hentsch for microscopy imaging, and S. Rousseau and staff at the ICS for ERG. We are grateful to E. Wagner (Vienna) for providing the JunAA mice. This work was supported by funds from INSERM and CNRS; European Community EUROSCA integrated project (LSHM-CT-2004- 503304), Hereditary Disease Foundation, the National Institutes of Health (EY011115 and EY007003), The Foundation Fighting Blindness, and Research to Prevent Blindness (RPB). J.S.F. is a recipient of a CIHR post-doctoral fellowship. A.S. is a Harold F. Falls Collegiate Professor and a recipient of RPB Senior Scientific Investigator award.

Appendix A. Supplementary data

Supplementary data associated with this article can be found, in the online version, at doi:10.1016/j.nbd.2006.11.002.

References

Abou-Sleymane, G., Chalmel, F., Helmlinger, D., Lardenois, A., Thibault, C., Weber, C., Merienne, K., Mandel, J.-L., Poch, O., Devys, D., Trottier, Y., 2006. Polyglutamine expansion causes neurodegeneration by altering the neuronal differentiation program. Hum. Mol. Genet. 15, 691–703.

Angel, P., Hattori, K., Smeal, T., Karin, M., 1988. The jun proto-oncogene is positively autoregulated by its product, Jun/AP-1. Cell 55, 875–885.

Behrens, A., Sibilia, M., Wagner, E.F., 1999. Amino-terminal phosphorylation of c-Jun regulates stress-induced apoptosis and cellular proliferation. Nat. Genet. 21, 326–329.

Bence, N.F., Sampat, R.M., Kopito, R.R., 2001. Impairment of the ubiquitin-proteasome system by protein aggregation. Science 292, 1552–1555.

Bessant, D.A., Payne, A.M., Mitton, K.P., Wang, Q.L., Swain, P.K., Plant, C., Bird, A.C., Zack, D.J., Swaroop, A., Bhattacharya, S.S., 1999. A mutation in NRL is associated with autosomal dominant retinitis pigmentosa. Nat. Genet. 21, 355–356.

Browne, S.E., Bowling, A.C., MacGarvey, U., Baik, M.J., Berger, S.C., Muqit, M.M., Bird, E.D., Beal, M.F., 1997. Oxidative damage and metabolic dysfunction in Huntington's disease: selective vulnerability of the basal ganglia. Ann. Neurol. 41, 646–653.

Chen, S., Wang, Q.L., Nie, Z., Sun, H., Lennon, G., Copeland, N.G., Gilbert, D.J., Jenkins, N.A., Zack, D.J., 1997. Crx, a novel Otx-like paired-homeodomain protein, binds to and transactivates photoreceptor cell-specific genes. Neuron. 19, 1017–1030.

Chen, G.K., Sale, S., Tan, T., Ermoian, R.P., Sikic, B.I., 2004a. CCAAT/enhancer-binding protein beta (nuclear factor for interleukin 6) transactivates the human MDR1 gene by interaction with an inverted CCAAT box in human cancer cells. Mol. Pharmacol. 65, 906–916.

Chen, S., Peng, G.H., Wang, X., Smith, A.C., Grote, S.K., Sopher, B.L., LaSpada, A.R., 2004b. Interference of Crx-dependent transcription by ataxin-7 involves interaction between the glutamine regions and requires the ataxin-7 carboxy-terminal region for nuclear localization. Hum. Mol. Genet. 13, 53–67.

Delhase, M., Castrillo, J.L., de la Hoya, M., Rajas, F., Hooghe-Peters, E.L., 1996. AP-1 and Oct-1 transcription factors down-regulate the expression of the human PIT1/GHF1 gene. J. Biol. Chem. 271, 32349–32358.

Di Figlia, M., Sapp, E., Chase, K.O., Davies, S.W., Bates, G.P., Vonsattel, J.P., Aronin, N., 1997. Aggregation of Huntingtin in neuronal intranuclear inclusions and dystrophic neurites in brain. Science 277, 1990–1993.

Dowling, J.E., 1987. The retina: an approachable Part of the Brain. Harvard University Press, Cambridge, MA.

Farjo, Q., Jackson, A., Pieke-Dahl, S., Scott, K., Kimberling, W.J., Sieving, P.A., Richards, J.E., Swaroop, A., 1997. Human bZIP transcription factor gene NRL: structure, genomic sequence, and fine linkage mapping at 14q11.2 and negative mutation analysis in patients with retinal degeneration. Genomics 45, 395–401.

Freund, C.L., Gregory-Evans, C.Y., Furukawa, T., Papaioannou, M., Looser, J., Ploder, L., Bellingham, J., Ng, D., Herbrick, J.A., Duncan, A., Scherer, S.W., Tsui, L.C., Loutradis-Anagnostou, A., Jacobson, S.G., Cepko, C.L., Bhattacharya, S.S., McInnes, R.R., 1997. Cone-rod dystrophy due to mutations in a novel photoreceptor-specific homeobox gene (CRX) essential for maintenance of the photoreceptor. Cell 91, 543–553.

Furukawa, T., Morrow, E.M., Li, T., Davis, F.C., Cepko, C.L., 1999. Retinopathy and attenuated circadian entrainment in Crx-deficient mice. Nat. Genet. 23, 466–470.

Garcia, M., Charvin, D., Caboche, J., 2004. Expanded huntingtin activates the c-Jun terminal kinase/c-Jun pathway prior to aggregate formation in striatal neurons in culture. Neuroscience 127, 859–870.

Grimm, C., Wenzel, A., Behrens, A., Hafezi, F., Wagner, E.F., Reme, C.E., 2001. AP-1 mediated retinal photoreceptor apoptosis is independent of N-terminal phosphorylation of c-Jun. Cell Death Differ. 8, 859–867.

Helmlinger, D., Yvert, G., Picaud, S., Merienne, K., Sahel, J., Mandel, J.-L., Devys, D., 2002. Progressive retinal degeneration and dysfunction in R6 Huntington's disease mice. Hum. Mol. Genet. 11, 3351–3359.

Helmlinger, D., Bonnet, J., Mandel, J.-L., Trottier, Y., Devys, D., 2004a. Hsp70 and Hsp40 chaperones do not modulate retinal phenotype in SCA7 mice. J. Biol. Chem. 279, 55969–55977.

Helmlinger, D., Abou-Sleymane, G., Yvert, G., Rousseau, S., Weber, C., Trottier, Y., Mandel, J.L., Devys, D., 2004b. Disease progression despite early loss of polyglutamine protein expression in SCA7 mouse model. J. Neurosci. 24, 1881–1887.

Helmlinger, D., Hardy, S., Sasorith, S., Klein, F., Robert, F., Weber, C., Miguet, L., Potier, N., Van-Dorsselaer, A., Wurtz, J.M., Mandel, J.-L., Tora, L., Devys, D., 2004c. Ataxin-7 is a subunit of GCN5 histone acetyltransferase-containing complexes. Hum. Mol. Genet. 13, 1257–1265.

Karin, M., 1995. lation of AP-1 activity by mitogen-activated protein kinases. J. Biol. Chem. 270, 16483–16486.

La Spada, A.R., Fu, Y.H., Sopher, B.L., Libby, R.T., Wang, X., Li, L.Y., Einum, D.D., Huang, J., Possin, D.E., Smith, A.C., Martinez, R.A., Koszdin, K.L., Treuting, P.M., Ware, C.B., Hurley, J.B., Ptacek, L.J., Chen, S., 2001. Polyglutamine-expanded ataxin-7 antagonizes CRX function and induces cone-rod dystrophy in a mouse model of SCA7. Neuron 31, 913–927.

Lahiri, D.K., Ge, Y., 2000. Electrophoretic mobility shift assay for the detection of specific DNA-protein complex in nuclear extracts from the cultured cells and frozen autopsy human brain tissue. Brai. Res. Brain Res. Protoc. 5, 257–265.

Lerner, L.E., Gribanova, Y.E., Ji, M., Knox, B.E., Farber, D.B., 2001. Nrl and Sp nuclear proteins mediate transcription of rod-specific cGMP-phosphodiesterase beta-subunit gene: involvement of multiple response elements. J. Biol. Chem. 276, 34999–35007.

Li, L., Fan, M., Icton, C.D., Chen, N., Leavitt, B.R., Hayden, M.R., Murphy, T.H., Raymond, L.A., 2003. Role of NR2B-type NMDA receptors in selective neurodegeneration in Huntington disease. Neurobiol. Aging 24, 1113–1121.

Lin, X., Antalffy, B., Kang, D., Orr, HT., Zoghbi, H.Y., 2000. Polyglutamine expansion down-regulates specific neuronal genes before pathologic changes in SCA1. Nat. Neurosci. 3, 157–163.

Lunkes, A., Lindenberg, K.S., Ben-Haiem, L., Weber, C., Devys, D., Landwehrmeyer, G.B., Mandel, J.-L., Trottier, Y., 2002. Proteases acting on mutant huntingtin generate cleaved products that differentially build up cytoplasmic and nuclear inclusions. Mol. Cell 10, 259–269.

Mathers, P.H., Grinberg, A., Mahon, K.A., Jamrich, M., 1997. The Rx homeobox gene is essential for vertebrate eye development. Nature 387, 603–607.

Mears, A.J., Kondo, M., Swain, P.K., Takada, Y., Bush, R.A., Saunders, T.L., Sieving, P.A., Swaroop, A., 2001. Nrl is required for rod photoreceptor development. Nat. Genet. 29, 447–452.

Merienne, K., Helmlinger, D., Perkin, G.R., Devys, D., Trottier, Y., 2003. Polyglutamine expansion induces a protein-damaging stress connecting heat shock protein 70 to the JNK pathway. J. Biol. Chem. 278, 16957–16967.

Miao, Z.H., Ding, J., 2003. Transcription factor c-Jun activation represses mdr-1 gene expression. Cancer Res. 63, 4527–4532.

Miller, V.M., Nelson, R.F., Gouvion, C.M., Williams, A., Rodriguez-Lebron, E., Harper, S.Q., Davidson, B.L., Rebagliati, M.R., Paulson, H.L., 2005. CHIP suppresses polyglutamine aggregation and toxicity in vitro and in vivo. J. Neurosci. 25, 9152–9161.

Molday, R.S., 1998. Photoreceptor membrane proteins, phototransduction, and retinal degenerative diseases. The Friedenwald Lecture. Invest. Ophthalmol. Vis. Sci. 39, 2491–2513.

Nishiguchi, K.M., Friedman, J.S., Sandberg, M.A., Swaroop, A., Berson, E.L., Dryja, T.P., 2004. Recessive NRL mutations in patients with clumped pigmentary retinal degeneration and relative preservation of blue cone function. Proc. Natl. Acad. Sci. U. S. A. 101, 17819–17824.

Nishitoh, H., Matsuzawa, A., Tobiume, K., Saegusa, K., Takeda, K., Inoue, K., Hori, S., Kakizuka, A., Ichijo, H., 2002. ASK1 is essential for endoplasmic reticulum stress-induced neuronal cell death triggered by expanded polyglutamine repeats. Genes Dev. 16, 1345–1355.

Owen, T.A., Bortell, R., Yocum, S.A., Smock, S.L., Zhang, M., Abate, C., Shalhoub, V., Aronin, N., Wright, K.L., van Wijnen, A.J., et al., 1990. Coordinate occupancy of AP-1 sites in the vitamin D-responsive and

CCAAT box elements by Fos-Jun in the osteocalcin gene: model for phenotype suppression of transcription. Proc. Natl. Acad. Sci. U. S. A. 87, 9990–9994.

Ozawa, Y., Nakao, K., Shimazaki, T., Takeda, J., Akira, S., Ishihara, K., Hirano, T., Oguchi, Y., Okano, H., 2004. Downregulation of STAT3 activation is required for presumptive rod photoreceptor cells to differentiate in the postnatal retina. Mol. Cell. Neurosci. 26, 258–270.

Pacione, L.R., Szego, M.J., Ikeda, S., Nishina, P.M., McInnes, R.R., 2003. Progress toward understanding the genetic and biochemical mechanisms of inherited photoreceptor degenerations. Annu. Rev. Neurosci. 26, 657–700.

Paulson, H.L., Perez, M.K., Trottier, Y., Trojanowski, J.Q., Subramony, S.H., Das, S.S., Vig, P., Mandel, J.L., Fischbeck, K.H., Pittman, R.N., 1997. Intranuclear inclusions of expanded polyglutamine protein in spinocerebellar ataxia type 3. Neuron. 19, 333–344.

Rattner, A., Sun, H., Nathans, J., 1999. Molecular genetics of human retinal disease. Annu. Rev. Genet. 33, 89–131.

Rehemtulla, A., Warwar, R., Kumar, R., Ji, X., Zack, D.J., Swaroop, A., 1996. The basic motif-leucine zipper transcription factor Nrl can positively regulate rhodopsin gene expression. Proc. Natl. Acad. Sci. U. S. A. 93, 191–195.

Ross, C.A., Poirier, M.A., 2004. Protein aggregation and neurodegenerative disease. Nat. Med. 10, S10–S17 (Suppl.).

Sandaltzopoulos, R., Becker, P.B., 1994. Solid phase DNase I footprinting: quick and versatile. Nucleic Acids Res. 22, 1511–1512.

Scherzinger, E., Lurz, R., Turmaine, M., Mangiarini, L., Hollenbach, B., Hasenbank, R., Bates, G.P., Davies, S.W., Lehrach, H., Wanker, E.E., 1997. Huntingtin-encoded polyglutamine expansions form amyloid-like protein aggregates in vitro and in vivo. Cell 90, 549–558.

Seong, I.S., Ivanova, E., Lee, J.M., Choo, Y.S., Fossale, E., Anderson, M., Gusella, J.F., Laramie, J.M., Myers, R.H., Lesort, M., MacDonald, M.E., 2005. HD CAG repeat implicates a dominant property of huntingtin in mitochondrial energy metabolism. Hum. Mol. Genet. 14, 2871–2880.

Shaulian, E., Karin, M., 2001. AP-1 in cell proliferation and survival. Oncogene 20, 2390–2400.

Sherman, M.Y., Goldberg, A.L., 2001. Cellular defenses against unfolded proteins: a cell biologist thinks about neurodegenerative diseases. Neuron 29, 15–32.

Skinner, P.J., Koshy, B., Cummings, C.J., Klement, I.A., Helin, K., Servadio, A., Zoghbi, H.Y., Orr, H.T., 1997. SCA1 pathogenesis involves alterations in nuclear matrix associated structures. Nature 389, 971–974.

Sohocki, M.M., Sullivan, L.S., Mintz-Hittner, H.A., Birch, D., Heckenlively, J.R., Freund, C.L., McInnes, R.R., Daiger, S.P., 1998. A range of clinical phenotypes associated with mutations in CRX, a photoreceptor transcription-factor gene. Am. J. Hum. Genet. 63, 1307–1315.

Swain, P.K., Hicks, D., Mears, A.J., Apel, I.J., Smith, J.E., John, S.K., Hendrickson, A., Milam, A.H., Swaroop, A., 2001. Multiple phosphorylated isoforms of NRL are expressed in rod photoreceptors. J. Biol. Chem. 276, 36824–36830.

Swaroop, A., Xu, J.Z., Pawar, H., Jackson, A., Skolnick, C., Agarwal, N., 1992. A conserved retina-specific gene encodes a basic motif/leucine zipper domain. Proc. Natl. Acad. Sci. U. S. A. 89, 266–270.

Trottier, Y., Lutz, Y., Stevanin, G., Imbert, G., Devys, D., Cancel, G., Saudou, F., Weber, C., David, G., Tora, L., Agid, Y., Brice, A., Mandel, J.-L., 1995. Polyglutamine expansion as a pathological epitope in Huntington's disease and four dominant cerebellar ataxias. Nature 378, 403–406.

Vacher, C., Garcia-Oroz, L., Rubinsztein, D.C., 2005. Overexpression of yeast hsp104 reduces polyglutamine aggregation and prolongs survival of a transgenic mouse model of Huntington's disease. Hum. Mol. Genet. 14, 3425–3433.

Warrick, J.M., Chan, H.Y.E., Gray-Board, G.L., Chai, Y., Paulson, H.L., Bonini, N.M., 1999. Suppression of polyglutamine-mediated neurodegeneration in Drosophila by the molecular chaperone Hsp70. Nature Genet. 23, 425–428.

Waza, M., Adachi, H., Katsuno, M., Minamiyama, M., Sang, C., Tanaka, F., Inukai, A., Doyu, M., Sobue, G., 2005. 17-AAG, an Hsp90 inhibitor, ameliorates polyglutamine-mediated motor neuron degeneration. Nat. Med. 11, 1088–1095.

Wenzel, A., Iseli, H.P., Fleischmann, A., Hafezi, F., Grimm, C., Wagner, E.F., Reme, C.E., 2002. Fra-1 substitutes for c-Fos in AP-1-mediated signal transduction in retinal apoptosis. J. Neurochem. 80, 1089–1094.

Whitfield, J., Neame, S.J., Paquet, L., Bernard, O., Ham, J., 2001. Dominant-negative c-Jun promotes neuronal survival by reducing BIM expression and inhibiting mitochondrial cytochrome c release. Neuron. 29, 629–643.

Wyttenbach, A., Sauvageot, O., Carmichael, J., Diaz-Latoud, C., Arrigo, A.P., Rubinsztein, D.C., 2002. Heat shock protein 27 prevents cellular polyglutamine toxicity and suppresses the increase of reactive oxygen species caused by huntingtin. Hum. Mol. Genet. 11, 1137–1151.

Yang, D.D., Kuan, C.Y., Whitmarsh, A.J., Rincon, M., Zheng, T.S., Davis, R.J., Rakic, P., Flavell, R.A., 1997. Absence of excitotoxicity-induced apoptosis in the hippocampus of mice lacking the Jnk3 gene. Nature 389, 865–870.

Yang, W., Dunlap, J.R., Andrews, R.B., Wetzel, R., 2002. Aggregated polyglutamine peptides delivered to nuclei are toxic to mammalians cells. Hum. Mol. Genet. 11, 2905–2917.

Yoo, S.Y., Pennesi, M.E., Weeber, E.J., Xu, B., Atkinson, R., Chen, S., Armstrong, D.L., Wu, S.M., Sweatt, J.D., Zoghbi, H.Y., 2003. SCA7 knockin mice model human SCA7 and reveal gradual accumulation of mutant ataxin-7 in neurons and abnormalities in short-term plasticity. Neuron. 37, 383–401.

Yoshida, S., Mears, A.J., Friedman, J.S., Carter, T., He, S., Oh, E., Jing, Y., Farjo, R., Fleury, G., Barlow, C., Hero, A.O., Swaroop, A., 2004. Expression profiling of the developing and mature Nrl−/− mouse retina: identification of retinal disease candidates and transcriptional regulatory targets of Nrl. Hum. Mol. Genet. 13, 1487–1503.

Yvert, G., Lindenberg, K.S., Picaud, S., Landwehrmeyer, G.B., Sahel, J.A., Mandel, J.-L., 2000. Expanded polyglutamines induce neurodegeneration and trans-neuronal alterations in cerebellum and retina of SCA7 transgenic mice. Hum. Mol. Genet. 9, 2491–2506.

Zhang, S.S., Liu, M.G., Kano, A., Zhang, C., Fu, X.Y., Barnstable, C.J., 2005. STAT3 activation in response to growth factors or cytokines participates in retina precursor proliferation. Exp. Eye Res. 81, 103–115.